Improve the long-term property of heat-cured mortars blended with fly ash by internal curing

Liu, Chen; Yang, Lu; Li, Zhenming; Nie, Shuai; Hu, Chuanlin; Wang, Fazhou

Important note
To cite this publication, please use the final published version (if applicable).
Please check the document version above.

Improve the long-term property of heat-cured mortars blended with fly ash by internal curing

Chen Liu [a,b,c], Lu Yang [a,*], Zhenming Li [c], Shuai Nie [a,b], Chuanlin Hu [a], Fazhou Wang [a,**]

[a] *State Key Laboratory of Silicate Materials for Architectures, Wuhan University of Technology, Wuhan, 430070, PR China*
[b] *School of Materials Science and Engineering, Wuhan University of Technology, Wuhan, 430070, PR China*
[c] *Department of Materials and Environment (Microlab), Faculty of Civil Engineering and Geoscience, Delft University of Technology, Delft, the Netherlands*

A B S T R A C T

Due to the satisfactory property and high productivity, heat-cured concretes have been widely used in engineering practice. However, heat curing process also brings some drawbacks that are detrimental to the long-term property of this material. To address this issue, lightweight fine aggregate (LWFA) was employed to provide internal curing (IC) for a heat-cured mortar (HCM) blended with fly ash (FA). The influences of LWFA on the interior relative humidity of HCM and the reaction environment and behavior of FA were measured. It was found that IC of LWFA could mitigate the drop of interior humidity and enhance the reaction degrees of cement and FA. This contributed significantly to the microstructure densification of HCM, higher compressive strength and better resistance to chloride ion. The results indicate that LWFA benefits to enhancing the efficiency of FA in a heat curing system and the combination of LWFA and FA contribute to improving the long-term property of HCM.

1. Introduction

Currently, precast concrete has been widely used in engineering infrastructures due to its high production efficiency and controllable properties. The heat curing technique is increasingly considered as a reliable and straightforward technique to meet the manufacturing requirements of precast concrete since it can rapidly enhance the early strength by accelerating early cement hydration [1–3]. However, the heat-cured concrete also suffers from some issues like uneven pore distribution and low long-term durability compared with standard-cured concrete. The main reason is that the rapidly formed hydrates at high temperatures can precipitate on the unhydrated cement particles and subsequently hinder the further hydration of inner cement particles [4–6]. Consequently, heat-cured mixtures commonly have superior early microstructure development but inferior long-term durability compared with standard curing regimes [7–9]. Based on this background, intensive methods have been conducted to enhance the long-term performance of heat-cured mortars, which can be generally divided into the following three aspects.

● Incorporation of supplementary cementitious materials (SCMs). FA, one of the most common SCMs, has been widely investigated and practiced in concrete manufacturing [10–18]. Due to its pozzolanic reactivity, FA can consume the portlandite generated by

cement hydration to promote the formation of "secondary hydration hydrates", which benefits to the long-term microstructure development of the matrix [19–22]. However, according to the literature [23–25], the addition of FA in heat-cured/steam-cured materials probably has no even adverse effect on the long-term properties. This can be attributed to the long-lasting low relative humidity of the concrete after heat curing. Due to the elevated temperature of curing condition, a large part of water in the matrix has been evaporated or consumed by cement hydration during the heat curing stage. Since water is the media for any chemical reaction, the reaction of FA in a heat-cured concrete will therefore be suppressed due to the lack of water at long-term ages. The adaptability of FA as well as other SCMs under heat curing condition is a significant issue that expects to be assigned further.

- Subsequent curing. There were many trials to enhance the long-term properties of heat-cured concretes by subsequent curing methods. Zou et al. [26] found that water curing and oven-dried curing could decrease the compressive strength and increase the surface permeability of steam-cured concrete significantly. Shi et al. [27] claimed that water curing was unrecommended to be used as a subsequent curing regime. Saturated lime water curing could improve the long-term properties of steam-cured concrete. The effects of ambient curing and sealed curing are in the middle of the above two ones. Actually, water curing is effective in a standard-cured system since it can supply external water to promote further cement hydration. However, the concrete after heat curing has already obtained a dense microstructure. The external water is more difficult to penetrate into a heat-cured concrete than in a standard-cured one at early ages [28]. In addition, the long-lasting soaking tends to dissolve hydrates such as portlandite [29], which will cause the deterioration of surface microstructure [30,31]. Generally, a relatively cost-efficient subsequent curing method for heat-cured concrete is sealed curing, but it still cannot better address the poor durability at long-term periods.

- Internal curing. IC has currently emerged as a promising technology that can produce concrete with increased resistance to early-age cracking and enhanced durability [32]. The primary objective of IC is to maximize hydration and minimize desiccation [32–40]. Subsequently, IC has been proved to reduce shrinkage and delay or eliminate unwanted cracking [41]. Due to the water storage requirement, agents used for IC need to have unique physical or chemical properties such as fiber, super absorbent polymer, lightweight aggregate [32,42–44]. Some plants or animal fibers from nature with a high specific surface area have both an internal curing effect and a toughening effect. Unfortunately, these natural fiber materials are commonly susceptible to temperature and become aged and invalid under heat curing conditions. Other than fiber, super absorbent polymer (SAP) is also a popular IC agent due to its unique chemical hydrophilic group. However, the water release of SAP will lead to shrinkage in volume, which leads to big gaps between SAP and matrix. Expanded shale, forming from the calcination of shales, is one type of LWFA and of great interest to use in concrete manufacturing. Due to the synergistic effect of IC and pozzolanic reactivity, this kind of aggregate can promote cement hydration and strongly strengthen the interfacial transition zone (ITZ) [36–40,45,46].

Although LWFA has achieved great success in a single cement system, the effect of LWFA on a binary system is rarely studied, especially under heat curing regimes. IC is promising to not only address the low relative humidity issue of heat-cured concrete at long-term ages but the low efficiency of FA in heat curing systems. To reduce the carbon footprint and enhance the long-term properties of FA-based HCM, employing 20% fly ash and 80% Portland cement as binder materials. The relative humidity of mortars and degrees of cement hydration were investigated to compare the hydration environment of FA with and without LWFA. The hydration behaviors of FA were examined by the reaction degree of FA, portlandite content and nuclear magnetic resonance (NMR). Compressive strength, resistance to chloride ions penetration, and water absorption test were also conducted to evaluate the long-term properties of HCM. The insights of work shed new light on the application of FA in heat curing regimes.

2. Experimental

Fig. 1 shows the schematic workflow of this work, which can be divided into three main parts. The first part was related to the property of LWFA comprising the chemical composition, phase assemblage and coordination chemistry of Si. Together with the density and water absorption rate of LWFA, physical and chemical properties of internal curing agent used in this work were clear. In the second part, several micro-scale tests were performed to understand the reaction environment and reaction behavior of FA in the IC condition supplied by LWFA. The last part regarding macro-scale characterizations was designed to measure water sorptivity, compressive strength and resistance to chloride ion of HCM mortars.
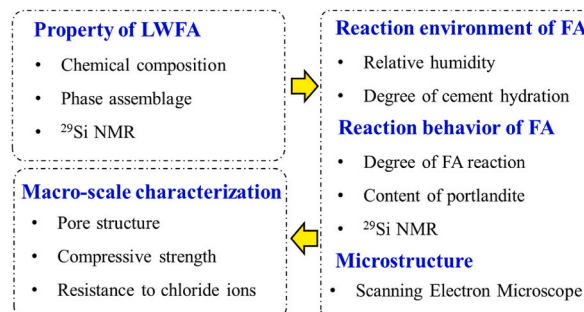

Fig. 1. Schematic workflow of this work.

2.1. Materials

The chemical properties of cement, FA, and LWFA used in this work are provided in Table 1. The gradation of sand ($\geq$98% quartz) and LWFA are shown in Fig. 2. The 24 h water absorption rate of LWFA was about 10% by mass, whose bulk density and absolute density (saturated surface dry condition) were 930 kg/m^3 and 1450 kg/m^3, respectively. The polycarboxylate-type superplasticizer was used to improve the fluidity of pastes.

Fig. 3 shows the chemical properties of LWFA used in this work. The LWFA used in this study was one type of aluminosilicate material called "expanded shale", in which silicon and aluminum accounted for more than 80%. A Bruker D8 Discover X-ray diffractometer with Cu(Kα) radiation was used to detect the phase assemblage of LWFA as shown in Fig. 3 (b). The primary mineralogical compositions were quartz and ringwoodite, and there was also a hump assigned to amorphous/glassy phases at the range between 15° and 35°. The content of glassy phases can be quantitatively determined by a selective chemical treatment with 20% HF, according to Refs. [47,48]. 10 g LWFA was dissolved in the solution of 200 mL of 20% HF in a plastic beaker and then stirred for 3 h at 40 °C, followed by vacuum filtration. The residue was washed by ethanol and dried for 6 h at 105 °C to a constant weight. The content of the glassy phase of LWFA was about 70.4%.

A Bruker MSL 400 spectrometer was employed to identify the coordination chemistry of Si in LWFA, as shown in Fig. 3 (c). The result shows that the main status of Si in both LWFA and FA was Q^4. Based on XRF, XRD and NMR measurements, the schematic of the chemical structure of LWFA can be depicted as Fig. 3. (d). The silicate and aluminum were the structural species forming the glassy skeleton of LWFA, while the R^{X+} (Fe^{3+}, Ca^{2+}, Mg^{2+}, Na^+, K^+) balanced the system charge. Fig. 3. (e) Shows the appearance of dry LWFA, whose pore structure is shown in Fig. 3. (f).

2.2. Preparation

The mortar mixtures were designed according to Ref. [32] in Eq. (1). An appropriate mass of water introduced by IC in the system should compensate the chemical shrinkage caused by binders. The mixtures are presented in Table 2. The chemical shrinkage for Portland cement is 0.07 mL/g, and FA can be two times greater [32]. The aggregate used in this work is about 55% of the mixture in volume.

$$C_f \times CS \times \alpha_{max} = S \times \Phi_{LWFA} \times M_{LWFA} \tag{1}$$

where C_f (g) is the mass of cementitious materials, CS (g/mL) is the chemical shrinkage of cementitious materials, α_{max} (unitless) is the expected maximum degree of cement hydration, Φ_{LWFA} (unitless) is the 24 h water absorption rate of LWFA, S (unitless, 100% in this work) is the expected degree of saturation of LWFA, and M_{LWFA} (g/cm^3) is the mass of LWFA in mixtures.

The specimen preparation was carried out at about 25 °C, and the heat curing regime is shown in Fig. 4. The red line represents the heat curing period (RH $\geq$ 98%), and the blue line represents the subsequent curing period (RH $\approx$ 55%).

2.3. Characterization

2.3.1. Relative humidity

The HC2–S humidity probe (Swiss-made), of which the accuracy is about $\pm$0.8% RH, was used in this work to monitor the relative humidity (RH) of internal HCMs. The setup is shown in Fig. 5. Before the test, fresh mortars were formed into a cylindrical mold (φ 100 mm $\times$ 200 mm), and a ventilated sleeve was inserted into the middle of the fresh mortar, then putting the probe into a sleeve. The part of the probe into slurries should be insulated and sealed by plastic film and aluminum tapes. Finally, using vaseline to seal the joint between the tape and film, after that, opening the temperature and humidity meters for data recording. The RH of the testing room was about 55%.

2.3.2. Selective dissolution

Selective dissolution is a technique aiming at dissolving the hydrates and the unhydrated clinkers without dissolving the unreacted FA [49]. The traditional dissolution agents are divided into two types: acids and complexants. The former type is (salicylic acid [50], picric acid [51], and hydrochloric acid [51]) based on acid-base neutralization. The latter one is used for chemically coupling with ions such as Ca^{2+}, Si^{4+}, Al^{3+}, Fe^{3+} and then decomposing the unwanted substance, among which ethylenediaminetetraacetic acid (EDTA), triethanolamine (TEA), diethylamine (DEA) are commonly used chemicals. According to previous literature [49], a solution consisting of EDTA, TEA and NaOH was optimized to determine the reaction degree of FA. The reaction degree of FA in this work follows the preceding solution of which the component is shown in Table 3.

Steps: First, the hydration-arrested sample was dried in an oven at 40 °C for 24 h, and then ground to pass through a 200 mesh square sieve. Second, 0.2 g sample powder (accurate to 0.0001 g) was weighed and dissolved into a prepared 200 mL selective solution (Table 3). The solution was ultrasonically placed and stirred with a glass rod for 10 min. Third, the solution was filtered

Table 1
Chemical properties of cement, FA and LWFA (wt%).

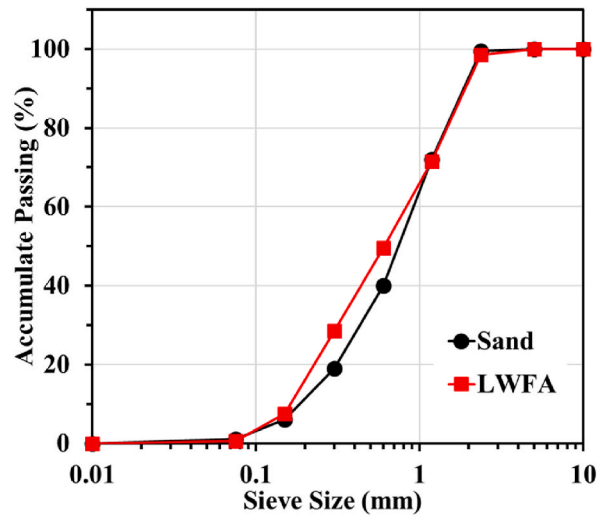|	Density (kg/m^3)	SiO$_2$	Al$_2$O$_3$	Fe$_2$O$_3$	CaO	MgO	K$_2$O	Na$_2$O	Others	Loss
Cement	3150	20.40	5.17	3.48	64.50	1.81	0.93	0.19	2.20	1.32
FA	2300	56.65	30.20	3.19	2.22	0.52	0.92	0.43	2.62	3.25
LWFA	1450	66.95	18.08	4.84	1.20	2.45	3.88	1.11	1.24	0.25

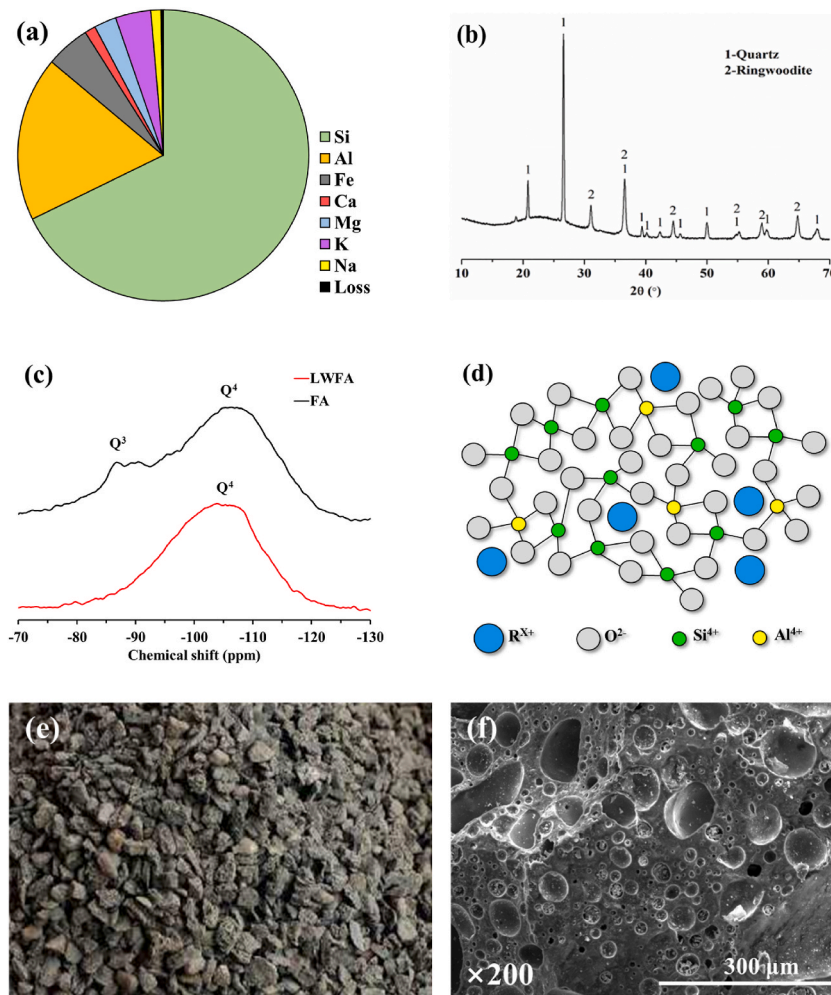**Fig. 2.** Gradation of sand and LWFA. (% by mass).

Fig. 3. Chemical properties of LWFA: (a) chemical composition; (b) XRD; (c) ^{29}Si NMR; (d) schematic of the amorphous phase of LWFA; (e) appearance of dry LWFA; (f) scanning electron microscopy image of pore structure of LWFA.

Table 2

Mixture proportions (kg/m³).

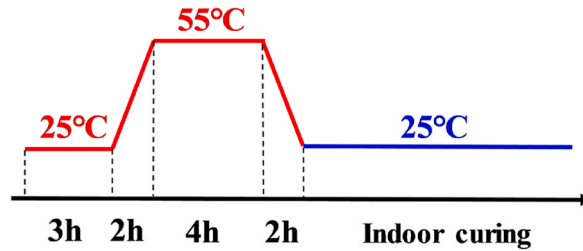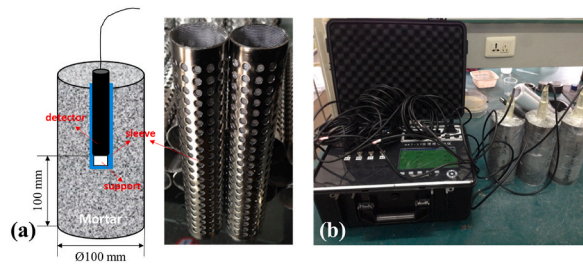|	Cement	FA	Sand	LWFA	Water	Superplasticizer
Blank	724	0	1352	0	217	5.79
FA	569	142	1327	0	213	5.69
LWFA	724	0	635	421	259	4.34
LWFA + FA	540	135	470	470	249	4.04

Fig. 4. Heat curing regime of HCM.

Fig. 5. Setup of relative humidity test.

Table 3

Chemical composition of selective solution (per liter).

	EDTA•H₂O	NaOH	TEA
Content	15.83 g	7.65 g	21.28 mL

through a 200 nm membrane. The beaker and glass rod was repeatedly washed with deionized water and ethanol. Lastly, the residue along with membrane was placed in a crucible and dried in an oven at 40 °C to constant weight. The mass loss before and after drying was recorded. Six replicates were conducted for each mixture.

Calculations: this part could be divided into binary and ternary systems. The binary one referred to the cement-FA and cement-LWFA systems, while the ternary one represented the cement-FA-LWFA system.

Binary system:

1 Normalization: this step was to remove the evaporated and chemical water in the dried sample at 40 °C for 24 h and then placed it in a furnace at 950 °C for 3 h. The calculation equations are shown in Eq. (2) and Eq. (3).

$$m_{S,N} = m_S(1 - f_W) \tag{2}$$

$$f_W = \left[m_{40} - \frac{m_{950}}{1 - LOI} \right] \Big/ m_{40} \tag{3}$$

where m_S is the initial mass of the sample, $m_{S,N}$ is the normalized mass of the sample, f_W (%) is the total water in the sample by mass, LOI (%) is the loss on ignition of the sample at 950 °C, m_{40} is the mass of the sample after drying at 40 °C for 24 h, m_{950} is the mass of the sample after furnacing at 950 °C for 3 h. All the mass is accurate to 0.0001 g.

2 Calculation of the mass of unreacted FA/LWFA in the residue

$$m_{FA-R/LWFA-R} = m_R - m_{S,N} \cdot f_C \cdot f_{RC} \tag{4}$$

where m_R is the mass of the residue, m_{FA-R} is the mass of the unreacted FA in residue, m_{LWFA-R} is the mass of the unreacted LWFA in residue, f_C (%) is the mass fraction of cement pastes, f_{RC} (%) is the mass fraction of residue of pure cement pastes after selective dissolution. All the mass is accurate to 0.0001 g.

3 Determination of FA/LWFA hydration degrees

$$\alpha_{FA/LWFA} = 1 - \frac{m_{FA-R/LWFA-R}}{m_{S,N} \cdot f_{FA/LWFA}}$$

$$\text{simplification:} \cdot \alpha_{FA/LWFA} = 1 + \frac{f_C}{f_{FA/LWFA}} \cdot f_{RC} - \frac{m_R}{f_{FA/LWFA} \cdot m_S \cdot (1 - f_W)} \tag{5}$$

where $f_{FA/LWFA}$ (%) is the mass fraction of FA/LWFA in pastes, $\alpha_{FA/LWFA}$ (%) is the reaction degree of FA/LWFA.

Ternary system:

1 Normalization: the same as the binary system, shown as Eq. (2) and Eq. (3).
2 Calculation of the mass of unreacted FA in the residue.

$$m_{FA-R} = m_R - m_{S,N} \cdot f_C \cdot f_{RC} - m_{S,N} \cdot (1 - \alpha_{LWFA}) \cdot f_{LWFA} \tag{6}$$

3 Determination of FA hydration degrees in HFC, which is simplified as Eq. (9)

$$\alpha_{FA} = 1 + \frac{f_C}{f_{FA}} \cdot f_{RC} + \frac{(1 - \alpha_{LWFA}) f_{LWFA}}{f_{LWFA}} - \frac{m_R}{f_{FA} \cdot m_S \cdot (1 - f_W)} \tag{7}$$

2.3.3. Calcium hydroxide content

Thermogravimetric analysis (TG) was employed to determine the content of calcium hydroxide (CH) in the paste. As reported [52], CH is decomposed at 400–500 °C while partially or fully carbonized portlandite is decomposed at 500–700 °C. The associated chemical reaction can be:

$$Ca(OH)_2 \rightarrow CaO + H_2O$$

$$CaCO_3 \rightarrow CaO + CO_2$$
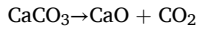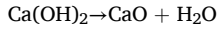
The mass of CH was calculated by Eq. (8):

$$m_{Ca(OH)_2} = \frac{74}{18} \Delta m_{400-500} \cdot + \frac{74}{44} \Delta m_{500-700} \tag{8}$$

where $m_{Ca(OH)_2}$ (g) is the mass of CH, $\Delta m_{400-500}$ (g) is the weight loss at 400–500 °C, $\Delta m_{500-700}$ (g) is the weight loss at 500–700 °C.

2.3.4. ^{29}Si NMR

To investigate the chemical coordination of Si in FA, LWFA and gels, ^{29}Si NMR test was conducted by a Bruker MSL 400 spectrometer. To reduce the interference of signal of aggregate impacting on the results as far as possible, the sand in HCM was removed without changing other components.

2.3.5. SEM

An FEI QUANTA FEG 450 scanning electron microscope (SEM) was employed to identify the morphology of FA in HCM pastes and microstructure of the interfacial transition zone (ITZ) between LWFA and pastes. The bulk samples were immersed in isopropanol to stop hydration and then dried at 40 °C for 2 h prior to testing. Besides, the sample for ITZ observation was well-polished with abrasive papers. An accelerating voltage of 20 kV and a working distance of 10 mm were selected for image capturing.

2.3.6. Degrees of cement hydration

Since LWFA is hard to detach from mortars, the degree of cement hydration was determined by the chemical bound water method [53]. The samples were dried at 105 °C for 24 h to remove nonchemical bound water and then placed at 1050 °C for 3 h to remove chemical bound water. The content of chemical bound water was calculated from the mass loss among 105 °C–1050 °C. In addition, the loss on ignition of cement, sand, and LWFA at 1050 °C was also considered. 1 g cement is assumed to require 0.25 g of water for complete hydration [54].

2.3.7. Strength and durability

2.3.7.1. *Sorptivity.* The sorptivity test was conducted to examine the pore structure of HCM. The preconditioning condition begins by first storing the samples at an environment with 50 ± 2 °C and 80 ± 2% (RH) for 3 days, and then drying at 23 ± 2 °C for 15 days based on ASTM C 1585 standard [55]. The average water absorption depth was calculated by Eq. (9):

$$I = \frac{m_t}{a \times \rho} \tag{9}$$

where I is the normalized water absorption, m_t is the mass change of specimen at time t (g), a is the area of specimen exposed to water (mm^2), and ρ is the density of water (10^{-3} g/mm^3).

According to some literatures [46,56], initial sorptivity and total sorptivity are measured as well, and the related formulas are shown as follows:

$$S_I = (m_I - m_D)/m_D \tag{10}$$

$$S_T = (m_S - m_D)/m_D \tag{11}$$

where S_I (unitless) is the initial sorptivity, S_T (unitless) is the total sorptivity, m_I (g) is the mass of specimens after preconditioning, m_D (g) is the mass of specimens after drying at 105 °C to constant weight, m_S (g) is the mass of specimens after 24 h vacuum water saturation.

2.3.7.2. Compressive strength. The compressive strength of HCM at 1, 7, 28, 60 d was measured by using a mechanical testing machine with a loading speed of 2.4 kN/s, according to NEN-196-1 [57].

2.3.7.3. Rapid chloride migration. The resistance to chloride ions is a significant parameter to evaluate the durability of cement concrete materials. The rapid chloride migration (RCM) test was measured based on NT Build 492 [58]. The migration coefficient was calculated by Eq. (12).

$$D_{RCM} = \frac{0.0239(273+T)L}{(U-2)t}\left(X_d - 0.0238\sqrt{\frac{(273+T)LX_d}{U-2}}\right) \tag{12}$$

where D_{RCM} is chloride migration coefficient ($\times 10^{-12}$ m^2/s); U is the initial absolute value of loaded voltage (V); T is the average value of initial and final temperature of the anolyte solution (°C); L is the thickness of specimen (mm); X_d is the average value of chloride migration distance (mm), and t is the test duration (h).

3. Results and discussion

3.1. Reaction environment of FA

3.1.1. RH of the internal HCM

Water is of great importance to both cement and FA reactions since water is the media of chemical reactions mostly. The RH of HCM with and without LWFA as an extension of time is shown in Fig. 6.

Generally, 60 days of testing time can be divided into three periods based on the gap of RH between two mortars: induction, acceleration, deceleration. During the first five days (stage I, induction), the gap of RH between two mortars is small. The RH of IC group is 2–3% higher than that without IC. Both of the two mortars maintain a high level of RH, which means water is sufficient for cement hydration at early stages. As the extension of hydration time, the gap constantly increases within 17 days (stage II, acceleration), indicating that IC takes effect at this stage. IC can effectively decrease the drop of RH by continually providing additional water to the system, which is conducive to cement hydration. However, after 17 days, the slop of the gap line considerably decreases (stage III, deceleration period) and the gap between two mortars reaches a plateau after 50 days. The RH of LWFA based HCM is 10–12% higher than that in the absence of LWFA in the long term. Therefore, it can be concluded in this test that IC can provide a more moist environment for cement. A high RH is probably beneficial for FA reaction.

3.1.2. Degree of cement hydration

Fig. 7 shows the degree of cement hydration within 60 days. It is evidently shown that the degree of cement hydration in both of two mortars increases as a function of time. Additionally, cement in LWFA-based HCM has a much higher reaction degree than that
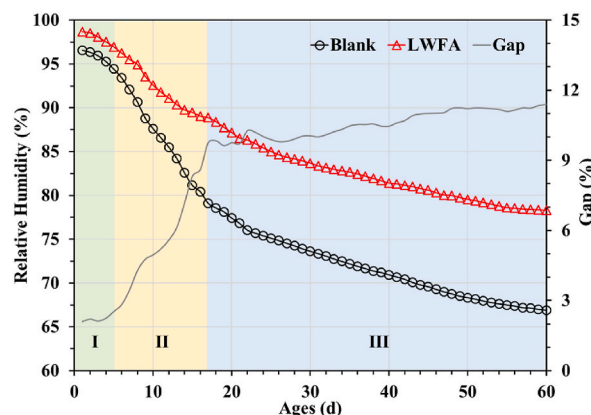

Fig. 6. RH of internal HCM.

without LWFA. This is mainly because the IC effect can provide unreacted cement particles with additional water to promote further hydration [24,35,50]. The degree of cement hydration with IC is about 10% higher than that of the pastes without IC at 60 d. A higher hydration degree of cement tends to form more cement hydrates and also more portlandite since it is a significant reaction product occupying about 15% in volume proportion in a Portland cement system. Furthermore, portlandite is a significant reactant in the pozzolanic reaction of FA, and the increased content of portlandite probably can promote the reaction of FA in HCM.

Combined with the RH and degree of cement hydration tests, the HCM with IC has a more moist hydraulic environment along with a higher content of portlandite (see section 3.2.2). All of this seems to indicate that IC can provide FA with a better hydraulic environment. The following section will focus on the reaction behavior of FA with and without IC.

3.2. Reaction behaviors of FA

3.2.1. Reaction degrees of FA

The reaction degree of FA in HCM determined by the selective dissolution method is shown in Fig. 8. It is found that FA in HCM blended with LWFA has a higher reaction degree than that without LWFA. More specifically, as shown in the grey line, reaction degrees of FA in LWFA-based mortar are 6.5%, 15.1%, 31.0% and 44.1% higher than the contrast group at 1 d, 7 d, 28 d, and 60 d, respectively.

The LWFA mainly has two positive effects on the reaction of FA. On one hand, pre-soaked LWFA can consecutively supply water to the system, which can promote ion transportation and the subsequent pozzolanic reaction of FA. On the other hand, as shown in section 3.1.2, the IC effect can enhance the hydration degree of cement, which means more portlandite are available in the LWFA-based system for FA reaction. Based on these two aspects, FA in the LWFA-based system has a higher reaction degree.

3.2.2. Content of CH

Fig. 9 (a) shows the TGA curves of different HCM at 60 d. The peaks of weight loss of gels (50–200 °C), CH (400–500 °C) and calcium carbonate (600–700 °C) are detected [52]. It is found that blank and FA groups have higher contents of both gels and CH than that in LWFA and LWFA + FA groups, which are mainly attributed to the dilution effect by the inclusion of LWFA. By the way, due to the indoor additional curing, carbonation is also identified in some of the samples. This part of calcium carbonation can be regarded as the carbonation of CH [59]. To better understand the impact of LWFA or/and FA on the cement hydration, the content of CH normalized by cement is calculated at different ages as shown in Fig. 9 (b). The content of CH in the blank group increases with time due to the continual cement hydration. However, the content of CH in pastes blended with FA or/and LWFA first increases and then decreases. Additionally, the value of LWFA and/or FA group is higher than that of the blank group before 28 days. For the FA-based group, due to its fine particle distribution and inert chemical reactivity, FA can provide sites for nucleation and thus accelerate cement hydration [60]. For the LWFA-based group, the increase of CH content is attributed to the IC effect of LWFA that can promote cement hydration. Therefore, the high content of CH in the LWFA group verifies the hypothesis proposed in section 3.2.1 that IC can promote the formation of CH.

Notably, the drops of CH at 60 d are observed in LWFA or/and FA pastes. This is mainly owing to the pozzolanic reaction at long-term ages. To better explain this result, a conceptual diagram associated with the relation between IC and pozzolanic reaction is proposed as shown in Fig. 10. As shown in section 3.1.1, the RH result presents that the water release of pre-soaked LWFA mainly occurs before 20 days, which means that the IC commonly takes effects at this period. Since the formation rate of CH is faster than the consumption rate (pozzolanic reaction), the content of CH in LWFA pastes is higher than the paste without LWFA before 28 d. However, as the deceleration of IC effect, the pozzolanic reaction becomes more and more evident. A hydraulic environment with high
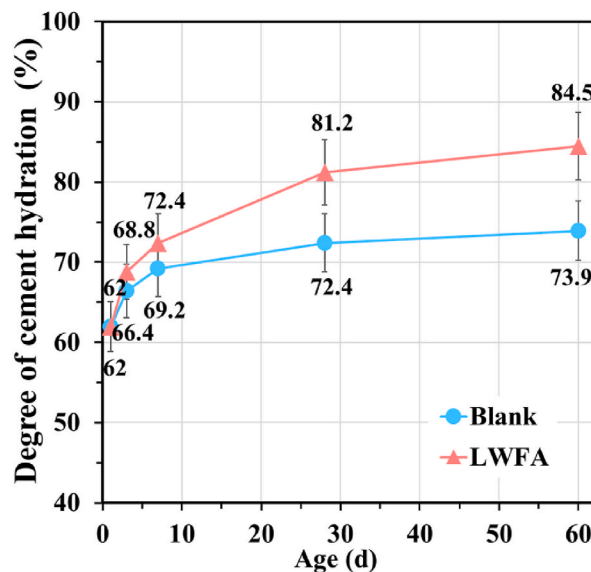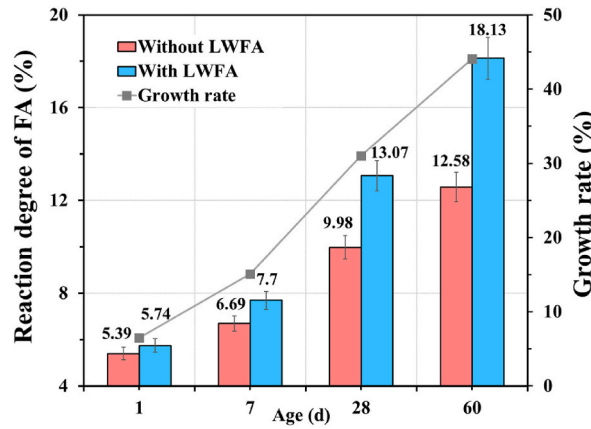

Fig. 7. Degrees of cement hydration.
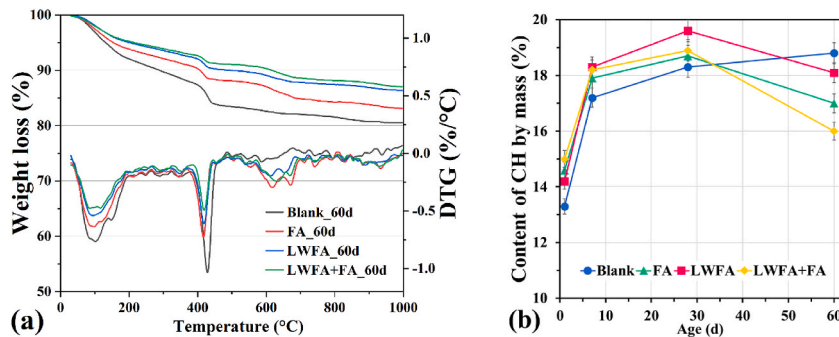
Fig. 8. Reaction degree of FA.

Fig. 9. TGA of HCM (a) TG and DTG curves of samples at 60 d (b) content of CH in HCM at different ages normalized by cement.
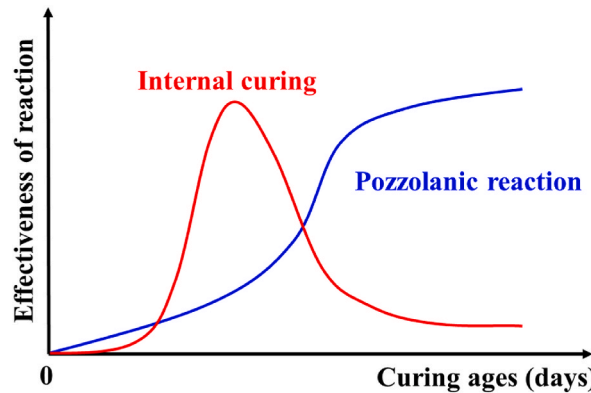

Fig. 10. A conceptual model of the relation between IC and pozzolanic reaction.

water and CH contents is beneficial to the decomposition of FA. Therefore, evident drops of CH are found in three blended systems, especially in the paste blended with LWFA and FA.

3.2.3. ^{29}Si NMR

To further understand the effect of LWFA on the reaction of FA, ^{29}Si NMR was conducted to identify the coordination chemistry of Si in HCM. Fig. 11 shows ^{29}Si spectra of FA-based mixtures with and without LWFA at 1 d and 60 d, respectively. According to the literature [61,62], five types of Si (Q^n, n = 0, 1, 2, 3, 4; n is the number of the bridge oxygen) can be classified in a Portland cement system. Among these, Q^0 represents the Si in unreacted clinker while Q^1 and Q^2 are assigned to the reaction products of cement and FA. The Si in LWFA and FA is referred to Q^3 and Q^4. It is observed that the signal of Q^0 significantly decreases and the reflection of Q^3 and Q^4 increases with the addition of LWFA. Besides, the comparison of each paste between 1 d and 60 d indicates that the content of Q^0, Q^3
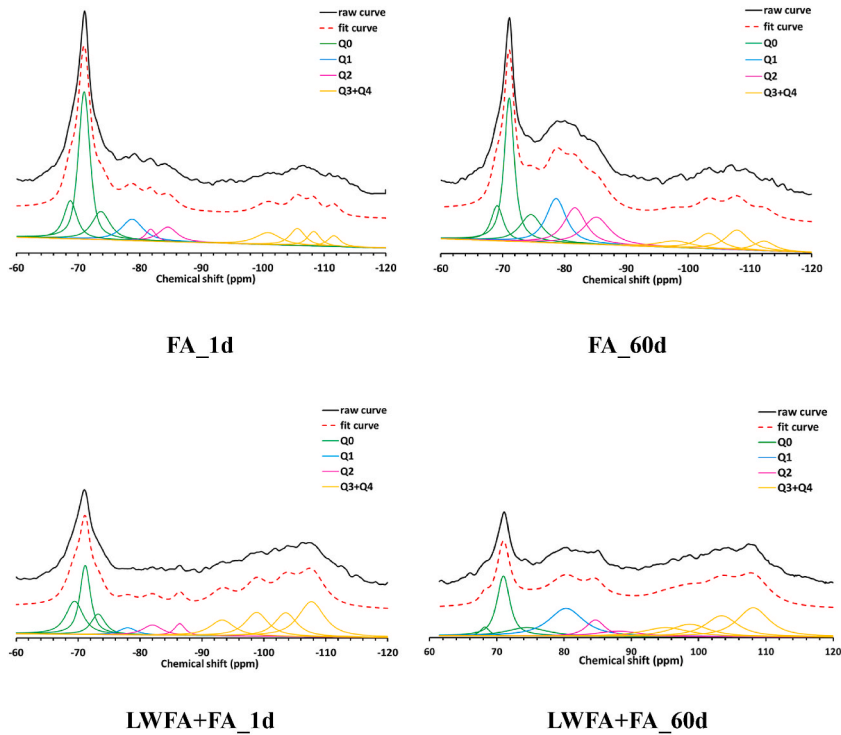
Fig. 11. ^{29}Si NMR spectra of FA-based mixtures with and without LWFA.

and Q^4 decreases with the increase of Q^1 and Q^2 content, which is attributed to the reaction of cement and FA.

Fig. 12 shows the content of Si in different chemical shifts, which are calculated from NMR results. After 60 days of reaction, the content of $Q^3 + Q^4$ in the pastes without LWFA decreases from 41.44% to 37.29%, while the LWFA-based paste decreases from 51.75% to 43.83%. This indicates that Si in Q^3 and Q^4 is much easier to be decomposed in the presence of LWFA. Integrated with the results shown in section 3.2.1 and 3.2.2, the NMR result provides more evidence that LWFA can promote the pozzolanic reaction of FA in HCM. It is plausible that a more thorough reaction of FA is conducive to long-term microstructure development and durability. A water absorption test is carried out to characterize the pore structure of HCM.

3.3. SEM

Fig. 13 shows the morphology of reacted FA and ITZ in LWFA-based HCM. It is observed that some linear reaction products lying on the surface of FA in view of the pozzolanic reaction of FA as shown in Fig. 13 (A). Since it can gain a better hydration environment with high RH and CH content with the presence of presoaked LWFA, FA in such condition have a higher reaction degree. The highly reacted FA is beneficial for the densification of ITZ which is commonly considered as the weakness zone in mortars and concretes. As shown in Fig. 13 (B), no evident dividing line is identified between the paste and LWFA, indicating that the ITZ between LWFA and paste is thin
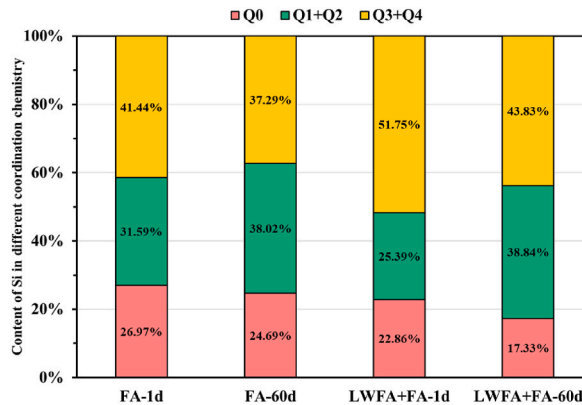

Fig. 12. Normalized deconvolution data of ^{29}Si NMR spectra of HCM.
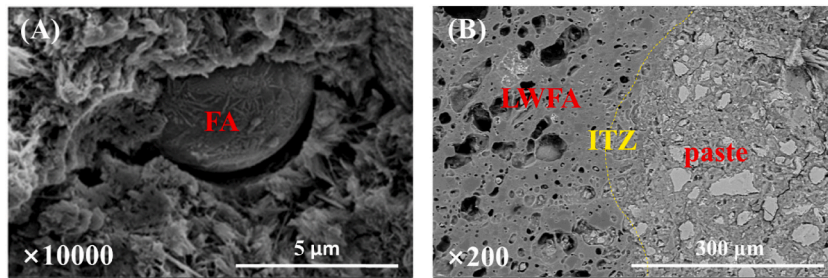
Fig. 13. Morphology of reacted FA and ITZ in HCM blended with LWFA at 60 d.

and dense. The densification of ITZ is of great significance to the diffusive transport of HCM [63]. The following water sorptivity test is conducted to examine the microstructure of different mortars.

3.4. Pore structure

A water sorptivity test was used to identify the pore structure of HCM [56,64]. Fig. 14 (a) and **(b)** show the total cumulative water absorption of HCM after 9 days. It is observed that the contrast group has the lowest water absorption rate among these four mortars, which means that neither LWFA nor FA is unable to improve the surface penetration property of HCM hydrated for 28 days. Since the pozzolanic reaction of FA and LWFA before 28 days doesn't work efficiently before 28 days, the binding of phase interfaces is weak and thus water can migrate in this porous structure readily. Moreover, it is noticed that the LWFA-based mortar has a much higher water absorption rate compared with the mortar without LWFA. A significant reason behind this is that the incorporation of LWFA introduces a lot of connected pores in the system. If the extra reaction products can not fully compensate for these connected pores introduced by LWFA, the water absorption rate will become higher than mortars without LWFA.

In contrast after 60 days, samples have considerably lower water absorption rates than that after 28 d. Additionally, the value of mortars significantly decreases with the employment of LWFA, among which HCM blended with LWFA and FA shows the lowest. As mentioned in the above section, IC can supply an excellent reaction environment, in which both cement and FA have higher reaction degrees. Thus, more hydration products are available to dense the structure of HCM.

Fig. 15 shows the open porosity and initial sorptivity of HCM at 28 d and 60 d, respectively. The combination of open porosity and initial sorptivity is considered as the total porosity of the mortar. It can be seen that the mortar with FA has a lower initial sorptivity compared with the pure cement group. In addition, due to the IC effect of LWFA, the LWFA-based mortar has higher initial water content. It is noticed that the total porosity of mortars blended LWFA is higher than that without LWFA. The major reason is that the total porosity is obtained from the mass of samples under a vacuum saturated condition, so most communication pores in the paste as well as the interior of LWFA can be filled under such condition. Therefore, water is hard to reach in that part of pores under a daily serving condition.

By the comparison of the water absorption and open porosity of HCM, a positive correlation between them can be found, as plotted in Fig. 16. The water absorption of HCM decreases with the decline of open porosity. This means the water absorption is strongly dependent on the open sorptivity. By the way, the lowest open porosity/water absorption of HCM blended with LWFA and FA among four mixtures at 60 d indicates that the synergistic effect of them can substantially the surface microstructure of HCM. Actually, the improvement of surface property is meaningful to the engineering practice of heat-cured materials since they commonly encounter the issue of thermal damage, especially the surface [65–67]. A dense surface microstructure is beneficial to not only the strength but also the resistance to ion penetration.

3.5. Compressive strength

Fig. 17 shows the compressive strength of HCM as a function of time. Since both the IC effect of LWFA and the pozzolanic reaction of FA work at long-term ages, HCMs blended with FA or/and LWFA show lower strength at early stages (1 d and 7 d) than that of the blank group. Despite, the compressive strength of LWFA-based mortars still reaches almost 40 MPa and 60 MPa at 1 d and 7 d, respectively. At 28 d, the compressive strength of all the HCM achieves varying degrees of enhancement, among which the growth of LWFA-based mortars is more notable. The value of LWFA and LWFA + FA groups at 28 d is 18.3% and 15.6% higher than that at 7 d. This indicates that the impact of IC has already taken effects at 28 d, but the contribution of pozzolanic effect of FA is not dominated within 28 d.

As an extension of curing ages, the compressive strength of HCM constantly increases. With the comparison of strength between 28 d and 60 d, it is observed that the effect of IC is still robust during this period. Meanwhile, the pozzolanic effect of FA plays growing importance on the development of compressive strength. The value of FA and LWFA + FA groups at 60 d increases by 20.9% and 33.1% compared with that at 28 d. This result is in agreement with the conceptual diagram shown in Fig. 10 that the pozzolanic reaction typically performs at long-term ages. With the presence of LWFA, HCM blended with FA shows the highest compressive strength after 60 days of curing ages, suggesting that FA in heat curing regimes can still make a great contribution to the mechanical property of HCM.
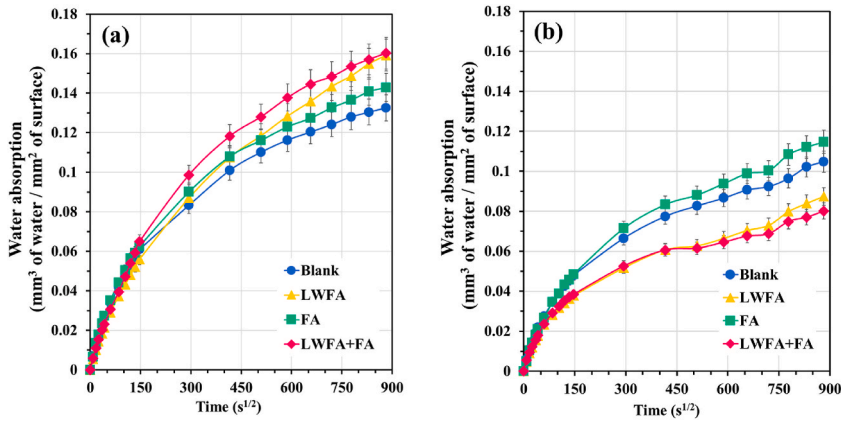
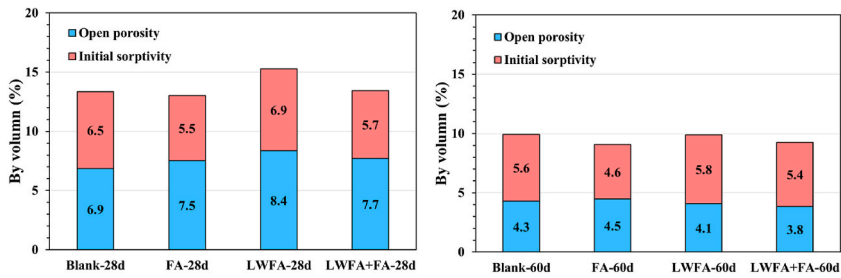**Fig. 14.** Cumulative water absorption of HCM cured for (a) 28 d and (b) 60 d.

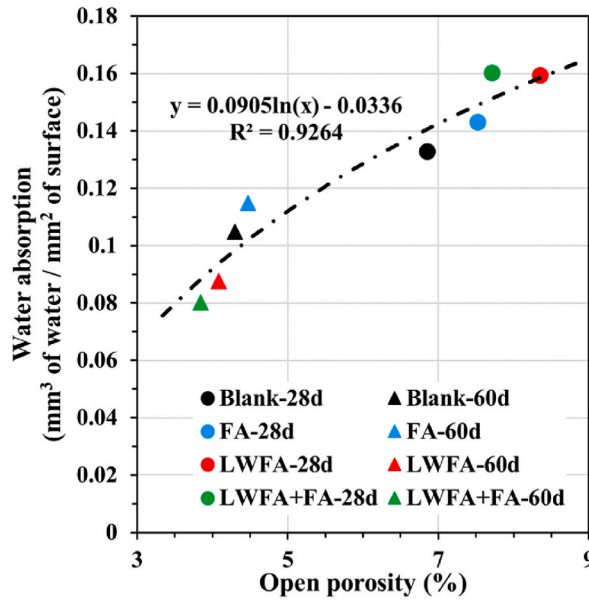**Fig. 15.** Sorptivity of HCM at different conditions.

Fig. 16. Relationship between water absorption and open porosity of HCM.

3.6. Resistance to chloride ions

Resistance to chloride ions is crucial to the durability of reinforced heat-cured concretes. Fig. 18 shows the rapid chloride migration coefficient of HCM at 28 d and 60 d. The HCM blended with LWFA shows lower migration coefficients at both 28 d and 60 d, which is consistent with some previous works [45,63,68,69]. The reason behind can be specified physically and chemically. On one hand, the IC
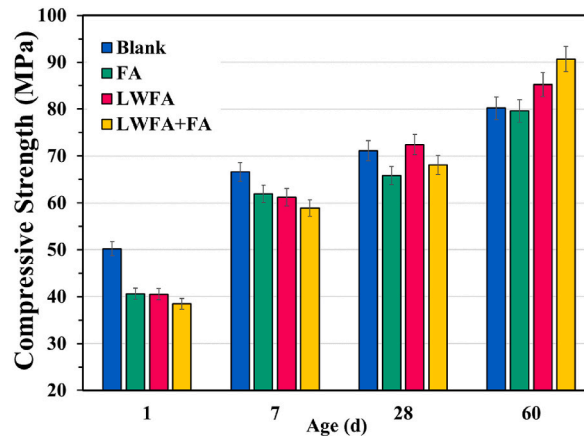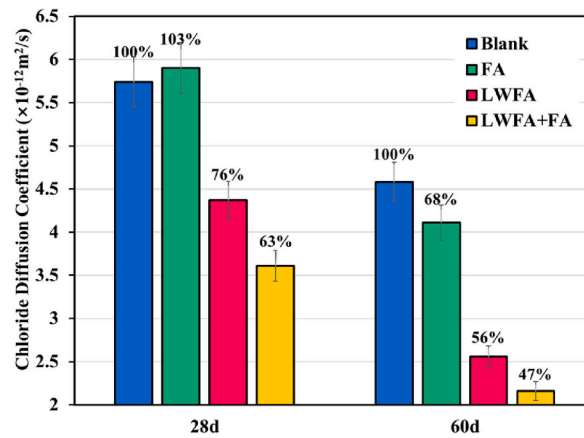
Fig. 17. Compressive strength of HCM.

Fig. 18. Rapid chloride diffusion coefficients of HCM.

effect can promote cement hydration and the formation of hydrates, which is conducive to obtaining a more thin and dense ITZ microstructure to prevent the mortar from ion attacks physically. On the other hand, the hydrates generated by the pozzolanic reaction of LWFA are also found to be effective in chemically binding the chloride ions [68,69].

It is noticed that the combination of LWFA and FA considerably decreases the chloride diffusion coefficients of HCM at 28 d and 60 d. FA in the system with IC has a more complete pozzolanic reaction, and the hydrates of FA reaction can not only dense the matrix but chemically bind chloride ions. Therefore, the joint use of LWFA and FA can enhance the long-term durability of HCM as well.

3.7. Summary

Based on the results mentioned above, the improvement of long-term properties of HCM can be attributed to the synergistic effect of LWFA and FA, as shown in Fig. 19. In this work, expanded shale as one kind of LWFAs was selected as the internal curing agent to prepare HCMs. The presoaked LWFA is considered as a small reservoir in the mortar, which can continually provide additional water during cement hydration. A higher RH of internal HCM is obtained with the incorporation of LWFA (Fig. 6). IC will promote cement hydration (Fig. 7) and the formation of reaction products such as CH (Fig. 9), which is the reactant of the pozzolanic reaction of FA. As a result, due to the water supplied by IC and more CH formed by increased cement hydration, FA in LWFA-based HCM has a higher reaction degree (Fig. 8). The IC effect and enhanced pozzolanic reaction of FA contribute to a great microstructure development of HCM. The water absorption rate (Fig. 14) and open porosity (Fig. 15) of mortars are significantly decreased in the presence of LWFA and FA. As a result, the long-term compressive strength and resistance to chloride ions are both improved by the synergistic effect of LWFA and FA.

This work, for the first time, quantitatively verifies that the IC of LWFA can promote the reaction of FA in heat-cured mortars. This suggests that the inclusion of pre-soaked LWFA is beneficial for the enhancement of the efficiency of FA under heat curing conditions. While the mortar blended with LWFA and FA has a poor strength and microstructure development at early ages, the long-term durability is highly improved by their coupling effect. The encouraging results also give valuable experience for a higher volume substitution of FA in heat-cured materials in the future.
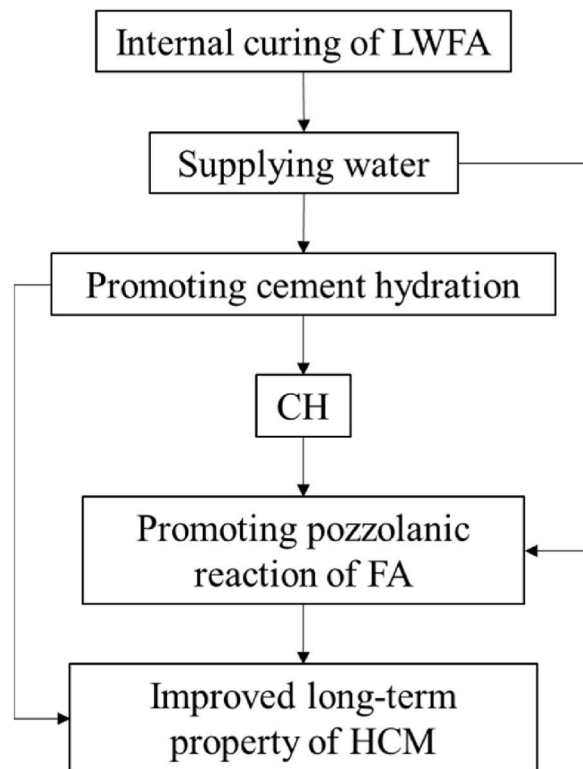
Fig. 19. Schematic diagram of the synergistic effect of LWFA and FA.

4. Conclusion

In this work, the incorporation of LWFA and FA was used to enhance the long-term properties of HCM. The impact of IC on the reaction environment of FA and the subsequent reaction behavior of FA are both investigated. Finally, the mechanisms of enhanced long-term properties of HCM blended with LWFA and FA are revealed. The following remarks can be clarified based on this study:

1. IC can increase the RH of internal HCM and the degree of cement hydration. The elevated cement hydration is beneficial to forming more CH that is of great importance to the pozzolanic reaction of FA. With a high RH and CH content reaction environment, FA in such condition obtains a higher reaction degree than that without IC.
2. The water sorptivity of HCM decreases in the presence of FA and LWFA, which is attributed to the synergistic effect of LWFA and FA. The improved reaction degrees of cement and FA are conducive to the formation of reaction products that can effectively dense the matrix and decrease the open porosity of HCM.
3. A dense microstructure contributes to the compressive strength and resistance to chloride ions of HCM. HCM blended with LWFA and FA shows superior long-term properties than the other mortars.
4. The adaptability of FA in a heat curing regime is improved by LWFA. The insight of this work is valuable for sustainable concrete production to achieve a higher volume clinker substitution by SCMs in heat-cured concrete without compromising long-term durability.

CRediT authorship contribution statement

Chen Liu: Conceptualization, Methodology, Investigation, Writing - Original Draft Preparation. Lu Yang: Supervision, Funding acquisition. Zhenming Li: Writing - Review & Editing. Shuai Nie: Investigation, Resources. Chuanlin Hu: Investigation. Writing - review & editing. Fazhou Wang: Supervision, Funding acquisition.

Declaration of competing interest

The authors declare that they have no known competing financial interests or personal relationships that could have appeared to influence the work reported in this paper.

Acknowledgments

References

[1] K.O. Kjellsen, R.J. Detwiler, Reaction kinetics of Portland cement mortars hydrated at different temperatures, Cement Concr. Res. 22 (1992) 112–120.

[2] K.O. Kjellsen, Heat curing and post-heat curing regimes of high-performance concrete: influence on microstructure and CSH composition, Cement Concr. Res. 26 (1996) 295–307.

[3] J.I. Escalante-Garcia, J.H. Sharp, Variation in the composition of C-S-H gel in Portland cement pastes cured at various temperatures, J. Am. Ceram. Soc. 82 (1999) 3237–3241.

[4] Q. Yang, Q. Yang, P. Zhu, Scaling and corrosion resistance of steam-cured concrete, Cement Concr. Res. 33 (2003) 1057–1061.

[5] F. Radjy, C.W. Richards, Effect of curing and heat treatment history on the dynamic mechanical response and the pore structure of hardened cement paste, Cement Concr. Res. 3 (1973) 7–21.

[6] H.-W. Reinhardt, M. Stegmaier, Influence of heat curing on the pore structure and compressive strength of self-compacting concrete (SCC), Cement Concr. Res. 36 (2006) 879–885.

[7] B. Lothenbach, F. Winnefeld, C. Alder, E. Wieland, P. Lunk, Effect of temperature on the pore solution, microstructure and hydration products of Portland cement pastes, Cement Concr. Res. 37 (2007) 483–491.

[8] F. Lin, C. Meyer, Hydration kinetics modeling of Portland cement considering the effects of curing temperature and applied pressure, Cement Concr. Res. 39 (2009) 255–265.

[9] C. Famy, K.L. Scrivener, A.K. Crumbie, What causes differences of CSH gel grey levels in backscattered electron images? Cement Concr. Res. 32 (2002) 1465–1471.

[10] G.P. Vagelis, Effect of fly ash on portland cement systems: Part II. High-calcium fly ash, Cement Concr. Res. 30 (2000) 1647–1654.

[11] M. Narmluk, T. Nawa, Effect of fly ash on the kinetics of Portland cement hydration at different curing temperatures, Cement Concr. Res. 41 (2011) 579–589.

[12] E. Sakai, S. Miyahara, S. Ohsawa, S.-H. Lee, M. Daimon, Hydration of fly ash cement, Cement Concr. Res. 35 (2005) 1135–1140.

[13] C.S. Poon, X.C. Qiao, Z.S. Lin, Pozzolanic properties of reject fly ash in blended cement pastes, Cement Concr. Res. 33 (2003) 1857–1865.

[14] Y.L. Wong, L. Lam, C.S. Poon, F.P. Zhou, Properties of fly ash-modified cement mortar-aggregate interfaces, Cement Concr. Res. 29 (1999) 1905–1913.

[15] C.Y. Lee, H.K. Lee, K.M. Lee, Strength and microstructural characteristics of chemically activated fly ash–cement systems, Cement Concr. Res. 33 (2003) 425–431.

[16] B. Lothenbach, K. Scrivener, R.D. Hooton, Supplementary cementitious materials, Cement Concr. Res. 41 (2011) 1244–1256.

[17] Z. Li, S. Zhang, X. Liang, G. Ye, Cracking potential of alkali-activated slag and fly ash concrete subjected to restrained autogenous shrinkage, Cement Concr. Compos. 114 (2020), 103767, https://doi.org/10.1016/j.cemconcomp.2020.103767.

[18] Z. Li, T. Lu, Y. Chen, B. Wu, G. Ye, Prediction of the autogenous shrinkage and microcracking of alkali-activated slag and fly ash concrete, Cement Concr. Compos. 117 (2021), 103913, https://doi.org/10.1016/j.cemconcomp.2020.103913.

[19] B. Szostak, G.L. Golewski, Rheology of cement pastes with siliceous fly ash and the CSH nano-admixture, Materials 14 (2021) 3640.

[20] G.L. Golewski, B. Szostak, Application of the CSH phase nucleating agents to improve the performance of sustainable concrete composites containing fly ash for use in the precast concrete industry, Materials 14 (2021) 6514.

[21] G.L. Golewski, B. Szostak, Strengthening the very early-age structure of cementitious composites with coal fly ash via incorporating a novel nanoadmixture based on CSH phase activators, Construct. Build. Mater. 312 (2021), 125426.

[22] G.L. Golewski, Green concrete based on quaternary binders with significant reduced of CO2 emissions, Energies 14 (2021) 4558.

[23] L. Baoju, X. Youjun, Z. Shiqiong, L. Jian, Some factors affecting early compressive strength of steam-curing concrete with ultrafine fly ash, Cement Concr. Res. 31 (2001) 1455–1458.

[24] B. Liu, Y. Xie, J. Li, Influence of steam curing on the compressive strength of concrete containing supplementary cementing materials, Cement Concr. Res. 35 (2005) 994–998.

[25] M.D.A. Thomas, Chloride diffusion in high-performance lightweight aggregate concrete, Spec. Publ. 234 (2006) 797–812.

[26] C. Zou, G. Long, C. Ma, Y. Xie, Effect of subsequent curing on surface permeability and compressive strength of steam-cured concrete, Construct. Build. Mater. 188 (2018) 424–432.

[27] J. Shi, B. Liu, S. Shen, J. Tan, J. Dai, R. Ji, Effect of curing regime on long-term mechanical strength and transport properties of steam-cured concrete, Construct. Build. Mater. 255 (2020), 119407, https://doi.org/10.1016/j.conbuildmat.2020.119407.

[28] N.S.V. Subramanian, Steam curing practice in the production of concrete sleepers: a study, Indian Concr. J. 70 (1996) 435–442.

[29] X. Li, W.Y. Niu, Effect of supplementary curing after steam-curing on performance of concrete, in: Mater. Sci. Forum, Trans Tech Publ, 2016, pp. 1376–1382.

[30] C. Carde, R. François, Effect of the leaching of calcium hydroxide from cement paste on mechanical and physical properties, Cement Concr. Res. 27 (1997) 539–550.

[31] R.R. Lloyd, J.L. Provis, J.S.J. Van Deventer, Pore solution composition and alkali diffusion in inorganic polymer cement, Cement Concr. Res. 40 (2010) 1386–1392.

[32] D.P. Bentz, W.J. Weiss, Internal Curing: a 2010 State-Of-The-Art Review, US Department of Commerce, National Institute of Standards and Technology, 2011.

[33] M.R. Geiker, D.P. Bentz, O.M. Jensen, Mitigating Autogenous Shrinkage by Internal Curing, ACI Spec. Publ., 2004, pp. 143–154.

[34] S. Zhutovsky, K. Kovler, A. Bentur, Efficiency of lightweight aggregates for internal curing of high strength concrete to eliminate autogenous shrinkage, Mater. Struct. 35 (2002) 97–101.

[35] M. Şahmaran, M. Lachemi, K.M.A. Hossain, V.C. Li, Internal curing of engineered cementitious composites for prevention of early age autogenous shrinkage cracking, Cement Concr. Res. 39 (2009) 893–901.

[36] M.-H. Zhang, O.E. Gjørv, Pozzolanic reactivity of lightweight aggregates, Cement Concr. Res. 20 (1990) 884–890.

[37] M.-H. Zhang, O.E. Gjørv, Microstructure of the interfacial zone between lightweight aggregate and cement paste, Cement Concr. Res. 20 (1990) 610–618.

[38] A. Elsharief, M.D. Cohen, J. Olek, Influence of lightweight aggregate on the microstructure and durability of mortar, Cement Concr. Res. 35 (2005) 1368–1376.

[39] S. Nie, S. Hu, F. Wang, P. Yuan, Y. Zhu, J. Ye, Y. Liu, Internal curing–a suitable method for improving the performance of heat-cured concrete, Construct. Build. Mater. 122 (2016) 294–301.

[40] C. Liu, Y. Liu, Z. Liu, C. Hu, X. Huang, L. Yang, F. Wang, Heat-cured concrete: improving the early strength and pore structure by activating aluminosilicate internal curing agent with triisopropanolamine, J. Am. Ceram. Soc. 102 (2019) 6227–6238.

[41] D. Shen, J. Jiang, J. Shen, P. Yao, G. Jiang, Influence of prewetted lightweight aggregates on the behavior and cracking potential of internally cured concrete at an early age, Construct. Build. Mater. 99 (2015) 260–271.

[42] P. Zhong, M. Wyrzykowski, N. Toropovs, L. Li, J. Liu, P. Lura, Internal curing with superabsorbent polymers of different chemical structures, Cement Concr. Res. 123 (2019), 105789.

[43] P. Jongvisuttisun, J. Leisen, K.E. Kurtis, Key mechanisms controlling internal curing performance of natural fibers, Cement Concr. Res. 107 (2018) 206–220.

[44] P. Lura, Autogenous Deformation and Internal Curing of Concrete, 2003.

[45] C. Liu, L. Yang, F. Wang, S. Hu, Enhance the durability of heat-cured mortars by internal curing and pozzolanic activity of lightweight fine aggregates, Construct. Build. Mater. (2020), 121439.

[46] S. Nie, W. Zhang, S. Hu, Z. Liu, F. Wang, Improving the fluid transport properties of heat-cured concrete by internal curing, Construct. Build. Mater. 168 (2018) 522–531.

[47] A. Fernández-Jimenez, A.G. De La Torre, A. Palomo, G. López-Olmo, M.M. Alonso, M.A.G. Aranda, Quantitative determination of phases in the alkali activation of fly ash. Part I. Potential ash reactivity, Fuel 85 (2006) 625–634.

[48] C. Li, Y. Li, H. Sun, L. Li, The composition of fly ash glass phase and its dissolution properties applying to geopolymeric materials, J. Am. Ceram. Soc. 94 (2011) 1773–1778.

[49] M. Ben Haha, K. De Weerdt, B. Lothenbach, Quantification of the degree of reaction of fly ash, Cement Concr. Res. 40 (2010) 1620–1629.

[50] K. Ogawa, H. Uchikawa, K. Takemoto, I. Yasui, The mechanism of the hydration in the system C3S-pozzolana, Cement Concr. Res. 10 (1980) 683–696.

[51] K. Luke, F.P. Glasser, Internal chemical evolution of the constitution of blended cements, Cement Concr. Res. 18 (1988) 495–502.

[52] Y.A. Villagrán-Zaccardi, H. Egüez-Alava, K. De Buysser, E. Gruyaert, N. De Belie, Calibrated quantitative thermogravimetric analysis for the determination of portlandite and calcite content in hydrated cementitious systems, Mater. Struct. 50 (2017) 179.

[53] G. Fagerlund, Chemically Bound Water as Measure of Degree of Hydration: Method and Potential Errors, Division of Building Materials, Lund Institute of Technology Lund, Sweden, 2009.

[54] K.O. Kjellsen, R.J. Detwiler, O.E. Gjørv, Development of microstructures in plain cement pastes hydrated at different temperatures, Cement Concr. Res. 21 (1991) 179–189.

[55] C. ASTM, 1585, Stand. Test Method Meas. Rate Absorpt. Water by Hydraul, ASTM Int., 2013, pp. 4–9.

[56] C. Astm, 1585-04, Standard Test Method for Measurement of Rate of Absorption of Water by Hydraulic-Cement Concretes, ASTM Int., 2004.

[57] B.S. En, Methods of testing cement—Part 1: determination of strength, Eur. Comm. Stand. Brussels, Belgium 169 (2005) 36.

[58] J. Lizarazo-Marriaga, J. Gonzalez, P. Claisse, Simulation of the Concrete Chloride NT Build-492 Migration Test, 2012.

[59] S. von Greve-Dierfeld, B. Lothenbach, A. Vollpracht, B. Wu, B. Huet, C. Andrade, C. Medina, C. Thiel, E. Gruyaert, H. Vanoutrive, I.F. Saéz del Bosque, I. Ignjatovic, J. Elsen, J.L. Provis, K. Scrivener, K.C. Thienel, K. Sideris, M. Zajac, N. Alderete, Ö. Cizer, P. Van den Heede, R.D. Hooton, S. Kamali-Bernard, S. A. Bernal, Z. Zhao, Z. Shi, N. De Belie, Understanding the Carbonation of Concrete with Supplementary Cementitious Materials: a Critical Review by RILEM TC 281-CCC, 2020, https://doi.org/10.1617/s11527-020-01558-w.

[60] B.W. Langan, K. Weng, M.A. Ward, Effect of silica fume and fly ash on heat of hydration of Portland cement, Cement Concr. Res. 32 (2002) 1045–1051.

[61] X. Gao, Q.L. Yu, H.J.H. Brouwers, Apply 29Si, 27Al MAS NMR and selective dissolution in identifying the reaction degree of alkali activated slag-fly ash composites, Ceram. Int. 43 (2017) 12408–12419.

[62] M.D. Andersen, H.J. Jakobsen, J. Skibsted, Characterization of white Portland cement hydration and the C-S-H structure in the presence of sodium aluminate by 27Al and 29Si MAS NMR spectroscopy, Cement Concr. Res. 34 (2004) 857–868, https://doi.org/10.1016/j.cemconres.2003.10.009.

[63] D.P. Bentz, Influence of internal curing using lightweight aggregates on interfacial transition zone percolation and chloride ingress in mortars, Cement Concr. Compos. 31 (2009) 285–289.

[64] B.B. Sabir, S. Wild, M. O'farrell, A water sorptivity test for martar and concrete, Mater. Struct. 31 (1998) 568.

[65] G. Long, Z. He, A. Omran, Heat damage of steam curing on the surface layer of concrete, Mag. Concr. Res. 64 (2012) 995–1004.

[66] J. Shi, B. Liu, F. Zhou, S. Shen, J. Dai, R. Ji, J. Tan, Heat damage of concrete surfaces under steam curing and improvement measures, Construct. Build. Mater. 252 (2020), 119104.

[67] Y. Xiang, G. Long, Y. Xie, K. Zheng, Z. He, K. Ma, X. Zeng, M. Wang, Thermal damage and its controlling methods of high-speed railway steam-cured concrete: a review, Struct. Concr. 22 (2021) E1074–E1092.

[68] M.V.A. Florea, H.J.H. Brouwers, Chloride binding related to hydration products: Part I: ordinary Portland Cement, Cement Concr. Res. 42 (2012) 282–290.

[69] A. Ipavec, T. Vuk, R. Gabrovšek, V. Kaučič, Chloride binding into hydrated blended cements: the influence of limestone and alkalinity, Cement Concr. Res. 48 (2013) 74–85.